Unraveling early events in the *Taphrina deformans – Prunus persica* interaction: an insight into the differential responses in resistant and susceptible genotypes

Running Title: *Prunus persica – Taphrina deformans* interaction

Laura A. Svetaz[14†], Claudia A. Bustamante[1†], Camila Goldy[15], Nery Rivero[1], Gabriela L. Müller[1], Gabriel H. Valentini[2], Alisdair R. Fernie[3] and María F. Drincovich[1] & María V. Lara[1]*

[†]Co-first author

[1]Centro de Estudios Fotosintéticos y Bioquímicos (CEFOBI). Facultad de Ciencias Bioquímicas y Farmacéuticas, Universidad Nacional de Rosario, Suipacha 531, 2000 Rosario, Argentina. [2]Estación Experimental San Pedro, Instituto Nacional de Tecnología Agropecuaria (INTA), Ruta Nacional nº 9 Km 170, San Pedro, Argentina; and [3]Planck-Institut für Molekulare Pflanzenphysiologie, Am Mühlenberg 1, 14476 Potsdam-Golm, Germany (A.R.F.).

Present addresses: [4]Farmacognosia, Facultad de Ciencias Bioquímicas y Farmacéuticas, Universidad Nacional de Rosario, Rosario, Argentina. [5]Instituto de Biología Molecular y Celular de Rosario (IBR-Consejo Nacional de Investigaciones Científicas y Técnicas), Facultad de Ciencias Bioquímicas y Farmacéuticas, Universidad Nacional de Rosario, Rosario, Argentina.

Correspondence: Dr. María Valeria Lara; lara@cefobi-conicet.gov.ar

This article has been accepted for publication and undergone full peer review but has not been through the copyediting, typesetting, pagination and proofreading process which may lead to differences between this version and the Version of Record. Please cite this article as doi: 10.1111/pce.12942

ABSTRACT

Leaf peach curl is a devastating disease affecting leaves, flowers and fruits caused by the dimorphic fungus *Taphrina deformans*. To gain insight into the mechanisms of fungus pathogenesis and plant responses, leaves of a resistant and two susceptible *P. persica* genotypes were inoculated with blastospores (yeast), and the infection was monitored during 120 hpi. Fungal dimorphism to the filamentous form and induction of ROS, callose synthesis, cell death, and defense compound production was observed independently of the genotype. Fungal load significantly decreased after 120 hpi in the resistant genotype while the pathogen tended to grow in the susceptible genotypes. Metabolic profiling revealed a biphasic re-programming of plant tissue in susceptible genotypes, with an initial stage co-incident with the yeast form of the fungus and a second when the hyphae is developed. Transcriptional analysis of *PRs* and plant hormone-related genes indicated that PR proteins are involved in *P. persica* defense responses against *T. deformans* and that salicylic acid is induced in the resistant genotype. Conducted experiments allowed the elucidation of common and differential responses in susceptible vs resistant genotypes, and thus allows us to construct a picture of early events during *T. deformans* infection.

Taphrina deformans is the causal leaf peach curl disease. For the first time fungal dimorphism from the yeast to the filamentous phase was achieved in inoculated P. persica leaves. Induction of ROS, callose synthesis, cell death, and defense compound production was observed in susceptible and resistant genotypes. Resistance against biotrophic T. deformans is associated with the activation of the salicylic acid- dependent pathway, induction of phenolics and up-regulation of defensin. A picture of early events during T. deformans infection is presented.

Keywords: Leaf curl disease, peach tree, biotrophic, dimorphism, salicylic acid, defensin, flavonoids

INTRODUCTION

Taphrina deformans (Berk.) Tul., is a biotrophic fungus causal of the "Leaf peach curl disease" (Mix, 1935) which in addition to leaves can also infect flowers and fruits. It is a devastating and economically important fungal pathogen of peach, nectarine and almond orchards in most of the cultivated areas of these species (Çmen & Ertugrul, 2007). In years of severe infection, leaves fall prematurely and this extensive defoliation corresponds to reductions in yields, higher susceptibility to frost and opportunistic pathogens, and even plant death (Pscheidt, 1995). In addition, infected fruits fall prematurely (Rossi *et al.* 2007).

Leaf peach curl disease is characterized by formation of tumor-like structures in leaves and fruits due to cell hyperplasia and hypertrophy (Mehrotra & Aneja, 1990). The disease appears at the beginning of spring as reddish areas in developing leaves. These areas got thicker and become curled. Subsequently, affected leaves turn brown or yellow and prematurely abscise (Rossi *et al.* 2007). Other symptoms include leaf spots, leaf curl, deformed fruits, and witches' brooms. It is proposed that plant hormonal imbalance due to phytopathogen infection is the cause of tumors due to the capacity of *T. deformans* to synthetize and excrete auxins, as well as cytokinins (Sziràki *et al.* 1975). That said, the exact mechanisms underlying tumor development remain, as yet, unclear (Tsai *et al.* 2014).

T. deformans is a dimorphic ascomycete. The filamentous form characterized by septate hyphae is exclusively found in its host (parasitic) while the yeast form is the saprophytic phase (Rodrigues & Fonseca, 2003). There is currently no information on the effectors that prompt the fungal dimorphism, which could be related either to host signals and/or to ploidy considerations (Nadal *et al.* 2008). Folial anatomy studies revealed that *T. deformans* grows intercellularly either below the cuticle and epidermis or among mesophyll cells. The

pathogen present on the lower surface penetrates though the stomata or into the cuticle. *T. deformans* does not form haustoria (Mix 1935). Thus, alteration of interface fungus-leaf cell wall allows pathogen growth. Transmission and scanning electron microscopy accompanied by histochemistry showed that the secretion of polysaccharide degrading enzymes such as cellulase by the hyphae growing in the intercellular spaces results in a partial dissolution of the plant cell walls. At the interface the cell wall texture is relaxed, the plant plasma membrane is markedly modified exhibiting vesiculation and the plant middle lamella is dissolved (Bassi *et al.* 1984). Although not tested, the dissolution of the middle lamella suggests the action of other lytic enzymes. In susceptible plants, other ultrastructural differences become evident on pathogen proliferation (Giordani *et al.* 2013).

The study of the resulting disease symptoms through anatomical approaches and of the climatologic conditions favoring the disease (Rossi et. al., 2007) has received most of the research attention invested in recent years. In contrast, little research has been conducted to elucidate the biochemical and molecular events involved in this interaction. Currently, with the availability of molecular methods that allow the identification of this fungus, there has been a renewed interest in the study of *T. deformans* – as demonstrated by the sequencing of its genome. The *T. deformans* genome encodes enzymes involved in plant cell wall degradation (cellulases, cutinases and xylanases) and many of the proteases which it encodes are predicted to be secreted (Cissé *et al.* 2013).

Resistance to this pathogen is rare; genotype screenings have classified either no or very few cultivars as tolerant (Pscheidt, 1995; Padula, 2008). Thus, understanding the molecular mechanisms underlying leaf peach curl disease resistance is critical to avoid economic losses. Bellini *et al.* (2002) in a program of controlled crosses analyzed more than two hundred genotypes. Then selected DOFI 71.043.018 ("Cesarini x Cesarini"), which was tolerant to *T. deformans*. After that, the progeny "DOFI-84.364" was obtained by self-pollination of DOFI

71.043.018 and then it was crossed with different resistant genotypes giving various selections. Such selection experiments are of great importance, not only to introduce resistance in commercial varieties but also to gain insight into the molecular events involved in the resistance against *T. deformans*, which are currently completely unknown. In the present work, a resistant advanced selection (DOFI-84.364.060) generated by Bellini and colleagues (2002) was investigated and results were compared with those of two susceptible genotypes.

In order to characterize the metabolic interactions that conduct to the disease establishment in susceptible plants or the responses involved in plant resistance in tolerant genotype, early events were examined. For this purpose, for the first time leaves of *P. persica* were inoculated with *T. deformans* in its yeast phase and the different phases of fungal colonization were followed up, which included the transition to the filamentous phase. A comprehensive analysis of plant defense responses was accompanied by metabolic profiling of inoculated leaves over a 120 h-period. Plant metabolome analyses successfully differentiated between resistant and susceptible genotypes and allowed to understand metabolic changes upon fungal inoculation. While the hypersensitive response was observed in all genotypes, differences in defense responses between resistant and susceptible genotypes were observed. Resistance against biotrophic *T. deformans* is associated with the activation of the salicylic acid (SA)- dependent pathway, induction of phenolics and up-regulation of defensin.

MATERIALS AND METHODS

Fungal and plant material

The yeast phase of *T. deformans* (PYCC 5894, Portuguese Yeast Culture Collection, Lisboa, Portugal) was kept on yeast malt agar medium (YMA; 0.3% (w/v) yeast extract, 0.5% (w/v) peptone, 1% (w/v) glucose, 0.3% (w/v) malt extract and 1.5 % (w/v) agar, pH 5-6) at 22 ºC.

Prunus persica L. Batsch trees from the advanced selections DOFI-84.364.089 and DOFI-84.364.060, generated by breeding in University of Florence (Bellini *et al.* 2002), and from cultivar Flavorcrest (FL), were grown at the Estación Experimental Agropecuaria INTA and monitored for at least five years. DOFI-84.364.089 (DS) and FL were classified as susceptible to *T. deformans* and DOFI-84.364.060 as resistant (DR).

Experimental Design and Inoculation

The inoculation of *T. deformans* onto *P. persica* leaves was performed with a blastospore suspension (9×10^6 blastospores.mL^{-1}) generated by dilution in H_2Od of 3-days old culture in YM. The abaxial surfaces of excised healthy leaves were inoculated with approximately 100 µL blastospore suspension and spreading the inoculum uniformly over the leaf surface. Inoculated leaves were sealed inside humid bags to ensure 100% RH and incubated in a chamber at 22ºC with 16-h light photoperiod for 120 h. Controls were conducted by spreading YM medium diluted in H_2Od at the same extent as blastopore suspension (mock). Inoculations were conducted under aseptic conditions. Inoculated leaves were harvested at 0, 6, 12, 24, 48, 72, 96 and 120 hours post inoculation (hpi) and used for histochemical staining procedures or frozen with $N_{2(l)}$ and kept at -80ºC for further use. Experiments were conducted at least three times (biological replicates) with at least three replicates each.

Histochemical staining procedures

Inoculated leaves were harvested at different time-points and clarified in ethanol. Samples were stained with aniline blue for visualization of callose and for staining of the fungal cell wall polysaccharides. Endogenous cell wall autofluorescence allowed the visualization of host tissue. The stained material was viewed with a microscope Nikon Eclipse TE-2000-E2 with confocal system Nikon C1Plus SiR using the following settings excitation = 405nm and emission = 450 nm. Images were acquired with the Nikon EZ-C1 software.

Accumulation of superoxide was visualized in vacuum infiltrated leaves with 0.5 $mg.mL^{-1}$ NBT (Nitroblue Tetrazolium, Promega) dissolved in buffer phosphate pH 6.8 as a dark blue insoluble formazan compound. Chlorophyll was removed from the leaves before imaging by boiling them in 95% (v/v) ethanol for 10 min.

The Evans Blue Staining method was used to evaluate cell death (Müller *et al.* 2010).

Pigment analysis

Carotenoids and flavonoids were quantified according to Müller *et al.* (2010). Phenolic compounds and anthocyanins were extracted and quantified as in Cantin *et al.* (2009).

Pathogen growth rate

DNA-based quantitative real time-PCR (qRT-PCR) method was used to analyze the growth of *T. deformans* in inoculated *P. persica* leaves. Fungal and plant DNA (DNAg) were extracted from peach leaves following the protocol described by Tavares *et al.* (2004). Ten nanograms of gDNA from *P. persica* inoculated leaves were used as a template in 20 µL reactions. qRT-PCR was run on the Agilent Mx3000P Real-Time System (Stratagene) and using the intercalation dye SYBRGreen I (Invitrogen) as a fluorescent reporter. The following settings were used: initial denaturation at 95°C for 3 min; 35 cycles at 94°C for 20 s, and 58°C for 20 s; 72°C for 1 min, and 72°C for 3 min. PCR primers ForTd

5’GGTCTCCGGATGGGTTTCAAG3’ and RevTd 5’GCATTTCGCTGCGTTCTTCA3’ were designed based on *T. deformans* internal transcribed spacer 1 (ITS1) sequence published in GenBank (AF492093.1) and using the program “primer3” (http://www.frodo.wi.mit.edu/cgibin/primer3/primer3_www.cgi). Assays were repeated with three different biological samples. Cycle threshold (Ct) value of *T. deformans* ITS1 gene was compared to plant elongation factor *1α* (*PpEF1α*, reference gene) in each sample for which the following primers were used: *EF1αFor* 5’ TCCAGTTCTTGATTGCCACA 3’ and 5′ *EF1αRev* 5’CCATACCTGCATCTTCGTTC 3’, and the relative value for *T. deformans* titer obtained using the comparative cycle threshhold method ($2^{-\Delta\Delta Ct}$). Amounts of *T. deformans* DNA were calculated using the standard curve constructed as follows.

For PCR sensitivity evaluation the concentration of fungal-DNA template required to obtain reproducible detection in three consecutive assays serial was evaluated. To define the limit of detection of the method ten-fold dilutions from 10 ng to 10 fg of fungal DNA template were employed. The average of the Ct values was calculated and plotted against the log of the DNA amount to construct the standard curves.

To evaluate the robustness of PCR in biological samples, the same curves described above were conducted with the addition of 10 ng of genomic DNA extracted from resistant plants (10 ng).

Gene expression analysis

Three μg of total RNA isolated from 40 mg leaves using the Trizol (Invitrogen) method, MoMLV-reverse transcriptase (Promega, Madison, WI, USA) and oligo(dT) were used for cDNA synthesis. Relative expression was quantified by qRT-PCR in an Agilent Mx3000P Real-Time System (Stratagene). Reactions, primer design, controls, PCR specificity confirmation, and relative gene expression calculation were conducted as exactly described in Lauxmann *et al.* (2014). Primers used are listed in Supporting Information Table S3. *PpEF1α*

was used as reference gene. Each assay was run in three technical replicates and repeated at least three times using different biological replicates.

Metabolite measurements

Metabolite profiling was assessed by Gas Chromatography–Mass Spectrometry (GC-MS) as described by Roessner-Tunali *et al.* (2003). Extraction was conducted as in Lauxmann *et al.* (2014) by using 100 mg of leaf. Ribitol was employed as internal standard. Mass spectra were cross-referenced with those in the Golm Metabolome Database (Kopka *et al.* 2005). Biological quintuplicates were performed for each stage (hpi) and genotype. Data sets were analysed by principal component analysis (PCA) and Pearson correlation analysis using XLSTAT package. For data representation MultiExperiment Viewer software (MeV v4.4.1, http://www.tm4.org/) was used. Data was normalized and expressed as log2 ratios to 0 hpi. Metabolite data is reported as Supporting Information according to Fernie *et al.* (2011) (Supporting Information Table S4).

Statistical analysis

Data were analysed using One Way Analysis of Variance (ANOVA). Minimum significance differences were calculated by the Bonferroni, Holm-Sidak, Dunett, or Fisher tests (α=0.05) using the Sigma Stat Package. To analyse whether differences among genotypes exist, Two Way ANOVA was also conducted.

RESULTS

Leaf inoculation and fungal dimorphism

To gain insight into the mechanisms of fungus pathogenesis and plant responses in the system *P. persica – T. deformans* we report, for the first time, inoculation experiments to follow the progress of infection. Leaves of a resistant (DOFI-84.364.060, DR) and two susceptible *P. persica* genotypes (DOFI-84.364.089, DS and Flavorcrest, FL) were

inoculated with *T. deformans* in its yeast phase and monitored during 120 h. Over the period analyzed, there were no macroscopic differences between mock and *T. deformans* inoculated leaves denoting that the pre-symptomatic phase is under study in this work (Supporting Information Fig. S1).

To follow the different phases of fungal colonization confocal microscopy was used (Fig. 1). *T. deformans* dimorphism from the yeast to the filamentous form was achieved after 48 hpi regardless the genotype inoculated (Fig. 1). Septated hyphae, typically of this ascomycete, were observed in all genotypes. In addition, in the section corresponding to a leaf from DS at 120 hpi it is illustrated how the fungus gained ingress into leaves through stomatal openings (Fig. 1); similar results were obtained with leaves of *P. persica* cv Flavorcrest (not shown). As expected, in control leaves from all genotypes no fungal development was observed, indicating that leaves were healthy before inoculation. In addition, there were no significant differences between the leaves of any genotypes before inoculation.

Besides monitoring infection by confocal microscopy, we developed an assay of quantitative real-time PCR to quantify the amount of *T. deformans* DNA in the inoculated leaves based on specific amplification of a fragment of *T. deformans* ITS1 gene and the comparison with that of *P. persica* EF 1α as an internal reference. Serial dilution (in water) and amplification of *T. deformans* genomic DNA using specific primers for ITS1 gene under the standard real time PCR conditions demonstrated that the PCR was able to detect 10 fg of fungal DNA (Fig. 2A, black circles). The sensitivity of the reaction was not significantly affected by addition of 10 ng of background plant DNA (Fig. 2a, gray squares). That is, there were no statistical significant differences ($P<0.05$) between the slopes of the standard curves conducted with and without the addition of plant DNA. Similarly, cycle threshhold (Ct)

values of plant EF1α (PpEF1α) were not influenced by addition of different amounts of fungal DNA (Fig. 2b).

After establishing the sensitivity and robustness of the assay, a calibration curve was constructed (Fig. 2c). Finally, total DNA extracted from *P. persica* leaves at different hours post inoculation with *T. deformans* was tested in each host genotype to measure the spread of the fungus (Fig. 2d). In both susceptible genotypes, a biphasic curve is observed, with a maximum at 24 hpi when the fungus is as yeast and then decreasing at 72 hpi and thereafter increasing from 96 hpi, when *T. deformans* is present in the filamentous form. In contrast, in the resistant DR, the amount of *T. deformans* only increases at 72 hpi, declining afterwards (Fig. 2d).

***P. persica* defense responses**

For the examination of the initial histological responses associated with *T. deformans- P. persica* interaction, superoxide production was evaluated histochemically in leaves challenged with *T. deformans*. As shown in Supporting Information Fig. S2, insoluble formazan blue deposition occurred in the three genotypes under study. Nevertheless, the increase in superoxide is earlier in leaves of DR (starting at 24 hpi) than in DS and FL. Evans blue-stained leaves were used to evaluate cell integrity during the 120 h period after inoculation. Cell death was visualized after 24 hpi in all the samples analyzed (Supporting Information Fig. S3). Neither differences among genotypes nor hpi were observed.

Aniline blue staining was used to disclose callose deposition (Fig. 1). Callose is a highly dynamic cell-wall component, frequently somewhat transient in nature. It is involved in a wide range of cell processes such as constituting a physical barrier at sites of infection that restricts the fungal spread (Chen & Kim, 2009). Intense fluorescence is observed in the epidermis of inoculated leaves (DS, DR, Fig. 1a and FL, not shown), with major regions of

fluorescence in guard cells, highlighting cell wall thickening around the stomatal pore. Qualitative analysis of images revealed no differences in the extent to which callose is deposited in resistant and susceptible genotypes. While some initial fluorescence is observed in mock-inoculated leaves (CDS), which may be a response to leaf detachment, the intensity decreases over the period analyzed. By contrast, fluorescence clearly increases over the time in the *T. deformans*-inoculated leaves.

The kinetics of pathogen induction of genes involved in plant defense responses was also explored. Genes encoding Pathogenesis Related (PR) proteins are commonly regulated by plants in pathogenic attacks (Van Loon *et al*. 2006). In addition, phenylpropanoid metabolism activation is key to secondary metabolite production of defense-related compounds, with Phenylalanine Ammonia Lyase (PAL) catalyzing the first committed step (Ferreira *et al.* 2007). Thus, based on literature on *Prunus* responding genes (Ziosi *et al.* 2008; Zubini *et al.* 2009; El-kereamy *et al.* 2011) and on plant defense in other species (Ferreira *et al.* 2007), an *in silico* analysis of *P. persica* genome was conducted to identify homologous genes in peach. Preliminary results allowed the identification of the genes expressed in *P. persica* leaves. Therefore, in this work the relative expression of transcripts encoding the following proteins, Lipid Transfer Protein 1 (LTP1, PR14), PAL1, Thaumatin Like Protein (TLP1, PR5), Catalase (CAT2), Defensin 1 (Dfn1, PR12) and Ribonuclease like Protein (Pp 1.06A, PR10) was assessed by qRT-PCR (Fig. 3). As controls, time course transcript relative expression was evaluated for most of the transcripts in mock-inoculated leaves to seek for putative changes independent of the fungal inoculation (CDR, Supporting Information Fig. S4). The pattern of accumulation of some transcripts in inoculated leaves was similar in all the *P. persica* genotypes (Fig. 3). While *PpTLP1* increases early after inoculation, *PpLTP1* greatly decreases; with both transcripts tending to increase at 120 hpi. Moreover, *PpCAT2* is not induced upon *T. deformans* inoculation in the three genotypes. By contrast, *PpDfn1* is

exclusively induced in the resistant genotype (DR) at 48 hpi, and *PpPR10* is differentially induced depending on the genotype showing significant rises at 6 and 72 hpi in FL, at 72 hpi in DR and at 120 in DS. Regarding *PpPAL1,* there is a significant increase at 72 hpi in DR, while in both susceptible genotypes DS and FL, *PpPAL1* is induced earlier and to a lesser extent (Fig. 3).

Hormonal responses are usually associated with either biotrophic or necrotrophic pathogens (Glazebrook, 2005). Thus, transcript levels of enzymes involved in various hormone biosynthetic pathways were also evaluated. The pattern of accumulation of Isochorismate synthase (*PpICS)* transcripts required for salicylic acid (SA) biosynthesis revealed a remarkable induction of almost twenty times at 96 hpi with respect to 0 hpi in the resistant plants (DR). Conversely, there was no induction of *PpICS* in DS over the period analyzed and a slight increase in FL at 120 hpi (Fig. 3). The expression of *PpACO1* (1-aminocyclopropane-1-carboxylate oxidase 1) was used as ethylene production marker. *PpACO1* was repressed in the resistant plants upon inoculation. By contrast, the transcripts were accumulated in the susceptible plants with a maximum of 38-fold in DS at 12 hpi, and of 2.7–fold in FL at 6 hpi (Fig. 3). Finally, *PpAOS* encoding an Allene oxide synthase (AOS) which is a key step in Jasmonic Acid (JA) synthesis was induced nearly two hundred times in FL at 72 hpi with respect to 0 hpi, and fifty times in DR with respect 0 hpi. Conversely, *PpAOS* decreased between 6 and 96 hpi in DS (Fig. 3). Collectively, these results suggest that SA may be involved in signaling events in the resistant genotype but not in the susceptible ones in response to *T. deformans*. Susceptible genotypes also exhibit a differential hormonal response, while ethylene would be induced in DS, JA would be activated in FL.

As means of evaluating plant defense responses, secondary metabolites, such as phenolic compounds (which include flavonoids and anthocyanins) and carotenoids were also quantified (Fig. 4). Total phenolics decreased in all genotypes during the first 24 hours. Nevertheless, resistant plants (DR) exhibited an induction at 96 hpi. Regarding anthocyanins, increases of 6- and 9.8-fold were observed at 12 hpi with respect to 0 hpi in DR and FL inoculated leaves, respectively. With respect to flavonoids, the higher levels of these compounds in leaves of DR before and after inoculation with respect to susceptible genotypes was notable; DR flavonoids at 0 hpi are about 2.5-fold the levels in DS. This fact notwithstanding, all genotypes show a maximum of flavonoids at 96 hpi (Fig. 4). On the other hand, carotenoids exhibited a rapid response, although of smaller magnitude, increasing in all genotypes at 6-12 hpi with a second peak being observed at 96 hpi (Fig. 4).

Primary metabolism in leaves of *P. persica* challenged with *T. deformans*

GC-MS analyses of leaves from the three genotypes (DR, DS and FL) resulted in the identification of 50 metabolites, which were grouped according their biochemical properties and functions as amino acids, organic acids, sugars, alcohol sugars, fatty acids or miscellaneous compounds. Amounts of each metabolite were determined in biological quintuplicates and estimated in relation to ribitol which was added as an internal standard. Normalized metabolite levels were expressed relative to the values measured in CDS (control leaves of non-inoculated DS) at each corresponding time after inoculation. Results are summarized in Supporting Information Table S1. Fig. 5 represents the relative metabolite levels and shows the changes in the metabolome with the time of inoculation. While some responses are common to all genotypes, as it is the case of miscellaneous compounds such as spermidine and urea, other variations are only shared by the susceptible genotypes (DS and FL), and not by DR, as it is the case of some sugars (raffinose and sucrose) and amino acids

(Asn, Trp and Tyr). In general and regardless the genotype, a biphasic response can be observed in the levels of all metabolites, with an early phase around 6 and 24 hpi and a later response centered at 96 hpi.

The metabolite profiles assessed by GC-MS were subjected to principal component analysis (PCA; Fig. 6) which showed the three highest-ranking principal components (PCs) accounted for 57.8% of the total variance within the data set. PC1, PC2 and PC3 accounted for 26.8%, 19.58% and 11.27% of total variance, respectively. PCA could clearly differentiate samples from susceptible genotypes (DS and FL) and those from the resistant plants (DR), especially in graphs PC1 vs PC2 and PC1 vs PC3. Supporting Information Table S2 depicts the contribution of individual variables to each principal component. Compounds that contribute the most to each component are shown in Fig. 6.

Metabolite-metabolite correlation analysis was pursued by using Pearson's correlation coefficients (Supporting Information Fig. S5). Out of 1225 pair-wise correlations, 422 resulted in significant correlation coefficients (P>0.5). While 308 coefficients of these were positive in nature, 114 were negative.

Metabolome analysis of leaves challenged with *T. deformans* revealed that in susceptible genotypes (DS and FL) the amino acids display a similar profile (Fig. 5 and 7) with two peaks of increase over the inoculation period. Among amino acids with this behavior, two groups can be distinguished. In the first group Asp, Glu, Ser, Thr and Val increase from 1.5- to 4-fold between 6- and 12 hpi and then show a second peak of 1.5- to 2-fold increase at 96 hpi. In the other group composed of Asn, Phe, Tyr and Trp, the second peak is closer to the first peak, at 48 hpi except for Asn that occurs at 24 hpi; in addition, this second group exhibits higher increases (between 5- and 80-fold). By contrast, in leaves of resistant plants (DR), neither an earlier induction (i.e. Asp, Ser, Thr, Val and Orn) nor change was observed. Moreover, the levels of most amino acids before inoculation (0 hpi) are considerable lower in

the resistant genotype DR than in susceptible plants (DS and FL, Fig. 7; i.e. Asp and Trp). On the other hand, Pro levels differs in the susceptible DS from FL and from DR (Fig. 5 and 7).

Regarding sugars, for some metabolites the same behavior is observed in both resistant and susceptible leaves, as it is the case of rhamnose and 1-O-methyl-manopiranoside. In other cases, such as fructose the tendency is to increase towards the end of the period analyzed. In the case of xylose, even though a net decrease is observed in all genotypes at 12 hpi, on one hand the relative levels in DR are higher than in both susceptible genotypes and tends to increase towards the end of the period analyzed. It is worth noting the case of raffinose which exhibits a substantial increase of between 30- and 80-fold in both susceptible genotypes (DS and FL) while DR display much lower levels at 0 hpi that remain constant or even decrease during the first days after inoculation (Fig. 5 and 7). Sugar alcohols also differ in susceptible plants than in the resistant genotype, as accounted by higher levels (between 2- and 4-fold higher) of glycerol-3-P in DS and FL than in DR over the period analyzed. On the other hand, in susceptible plants galactinol doubles (in DS) or triples (in FL) its level at 12 hpi with respect to 0 hpi (Fig. 5 and 7).

In the organic acid module, benzoate, 4-amine-butyrate (GABA) and fumarate levels exhibit two peaks across the inoculation period but do not display genotype effects. Regarding glycerate, an early peak at 6 hpi is observed in the three genotypes; and a second increase of 2.7-times is registered only in DR at 96 hpi. On the other hand, citrate depicts a peak at 96 hpi, which is of higher magnitude in susceptible plants than in DR (4.3-, 2.1- and 1.4– fold increase with respect to 0 hpi in DS, FL and DR, respectively). Conversely, malic, quinic and *trans*-caffeic acids differ in resistant plants with respect to susceptible ones. Particularly, malate increases 2- and 3-fold in DS and FL, respectively at 12 hpi; while the resistant plants induction of about four times with respect to 0 hpi occurs later at 96 hpi (Fig. 5 and 7).

Despite mild variations in the fatty acids profile, there were no remarkable differences unique to the susceptible or resistant plants (Fig. 5 and 7).

Regarding the miscellaneous compounds, chlorogenic acid (*cis*-3-caffeoyl-quinic acid) increases about two fold at 12 hpi with respect to 0 hpi and then tends to increase later in all genotypes although at different extent. Spermidine also tends to increase in all genotypes as well, but returns to initial levels at 120 hpi. Although urea depicts a similar profile in all genotypes analyzed, the initial decrease in the susceptible plants is not observed in DR (Fig. 5 and 7).

Finally, since raffinose was dramatically induced in susceptible genotypes (DS and FL) upon *T. deformans* inoculation, a comprehensive profiling of transcripts encoding enzymes involved in its metabolism was conducted by qRT-PCR (Fig. 8). In the first step of raffinose biosynthesis, galactinol synthase (GolS) produces galactinol, which is then used by raffinose synthase (RS) to produce the trisaccharide. By contrast, the so-called "Seed Imbibition Proteins (SIPs)" are –galactosidases involved in raffinose catabolism (Lauxmann *et al.* 2014). Time course of transcript expression in FL revealed no significant changes in *PpGolS1* and *PpRS* over the 120 hpi analyzed, increases in *PpGolS4* at 72, 96 and 120 hpi, a slight increase of *PpSIP1* at 24 hpi, and a significant decrease of *PpSIP2* upon inoculation with relative values ranging from 5 and 33% of that at 0 hpi. A complete different profile was observed in DS; with a two-fold increase in *PpRS* at 12 hpi, a significant fall in both *PpGolS-1* and *-4* upon pathogen inoculation and a prominent induction of both *PpSIP-1* and *-2* around 72 and 96 hpi (Fig. 8). Regarding the resistant plant, while *PpGolS4* increased at 6 hpi, *PpGolS1* decreased at the same time and remained low, *PpRS*, *PpSIP-1* and *-2* remained almost constant over the period analyzed (Fig. 8).

Given that Pro accumulated to a great extent in DR and FL, transcripts encoding the enzymes involved in the synthesis of its precursor Pyrroline-5-carboxylate (P5C), P5C synthase (*PpP5CS-1* and *-2*) and δ-ornithine aminotransferase (*Ppδ**OAT*), were quantified in both susceptible and resistant plants (Fig. 8). In DR, while *Ppδ**OAT* remained constant, *PpP5CS-1* and *-2* showed increases at 6 hpi (four-fold with respect to 0 hpi) and 72 hpi (ten-fold with respect to 0 hpi), respectively. Surprisingly, in FL *Ppδ**OAT, PpP5CS-1* and *-2* declined after *T. deformans* inoculation. Regarding DS, *Ppδ**OAT* (twelve-fold) and *PpP5CS1* (seven-fold) were induced at 12 hpi with respect to 0 hpi, and a second peak at 96 hpi was observed for *PpP5CS1* at 96 hpi. *PpP5CS2* did not exhibit significant changes (Fig. 8).

DISCUSSION

The filamentous form of *T. deformans* is developed in *P. persica* leaves after inoculation with the yeast phase

Taphrina deformans is the causal agent of Peach Leaf Curl, a disease that not only affects peach and nectarine but also almond orchards around the world (Rossi *et al.* 2007). It is a harmful pathogen that causes important economical loses; however, the dimorphic nature of this fungus has constituted an hindrance to knowledge enlargement of this disease. To understand the interaction between *T. deformans* and its host *P. persica*, a comprehensive analysis of the fungal development and the plant metabolic response was conducted here. Even though all known commercial cultivars are susceptible to this pathogen, an advanced selection breeding approach to yield a resistant line (DOFI-84.364.060) was performed in Italy (Bellini *et al.* 2002) and this line was used in the current work to obtain insight into the factors underlying resistance. On the other hand, to ascertain the metabolic changes associated with pathogen colonization and to discriminate them from biological variation,

two susceptible genotypes were employed, Flavorcrest and DS (another member of the same selection panel as DR). The aim of this study was to achieve a deep characterization of the early responses upon pathogen inoculation, and thus analyze the pre-symptomatic stage of the disease. The absence of leaf hyperplasia or changes in pigmentation in treated leaves (Supporting Information Fig. S1) are evidence that signs of disease are not yet developed during the period analyzed. To the best of our knowledge, this is the first time that *P. persica* leaves are inoculated with *T. deformans* and the progress of infection and plant responses are evaluated during the following 120 hours and that fungal dimorphism has been achieved under laboratory conditions. Regardless of the plant genotype, septated hyphae were visualized after 48 hpi (Fig. 1). Many economically important pathogens are dimorphic fungus such as *Magnaphorthe grisea* infecting rice, wheat, barley, rice, etc.; *Ustilago maydis* infecting maize and *Mycosphaerella graminicola* affecting wheat (Doehlemann *et al.* 2008; Nadal *et al.* 2008; Gohari *et al.* 2015; Mc Donald *et al.* 2015; Rudd *et al.* 2015; Lo Presti *et al.* 2015; Tollot *et al.* 2016). *U. maydis* has become a model species to study fungal pathogenicity and dimorphism. For many of these dimorphic fungi the transition to the pathogenic state can be mimicked in culture by media modification (Guevara-Olvera *et al.* 1997; Nadal *et al.* 2008). In the case of *T. deformans* stable hyphal development occurs exclusively in the host tissue and thus, filamentous form is considered as obligate parasitic. Therefore, the establishment of a system that allows the hyphae development under controlled laboratory conditions is of great importance.

In comparison with other biotrophs such as *U. maydis*, a pathogen that forms the specialized haustoria for nutrition and grows both inter- and intra-cellularly, the induction of *T. deformans* dimorphism is more slowly. While after 12 hpi, most of the *U. maydis* haploid sporidia used to infect maize had formed hyphae and developed the appresosoria (Doehlemann *et al.* 2008), only after 48 hpi *T. deformans* yeast cells had turned into their

filamentous form. On the other hand, in both maize-*U. maydis* and *P. persica*- *T. deformans* pathosystems early plant responses are observed around 12 hpi (Doehlemann *et al.* 2008, Figs. 4, 5, 7 & 8).

Early responses are activated in *P. persica* in response to *T. deformans* inoculation

Plants safeguard themselves by means of both biochemical and physical defenses. During early stages of pathogen invasion production of reactive oxygen species (ROS) and defense compounds by host tissue is usually accomplished. Here, the superoxide anion accumulated upon *T. deformans* inoculation in all genotypes, this was also accompanied by cell death, with both features indicative of a hypersensitive response (HR, Supporting Information Fig. S2 and S3). In addition, callose deposition was also observed (Fig. 1).

The analysis of the transcriptional responses of genes involved in the biosynthesis of hormones that usually respond to pathogen attack reveals an early induction of *PpAOS* followed by a later activation of *PpICS* in DR to *T. deformans* infection (Fig. 3). Resistance against biotrophic pathogens is frequently regulated by salicylic acid (SA), whereas jasmonate and ethylene-dependent pathway activation are usually associated with resistance to necrotrophic pathogens (Bari & Jones, 2009). In DR, *PpICS* induction at 96 hpi parallels the decrease in *T. deformans* (Fig. 2). Since SA acts locally and systemically (Vlot *et al.* 2009), activation of SA synthesis through isochorismate synthase may be efficient against the filamentous form of *T. deformans* and also facilitate Systemic Acquired Resistance in the DR genotype and thus mediate the defense in distal parts of the plant. By contrast, SA appears not to be induced in the FL and DS, a condition that is thus conducive to the disease. In the susceptible genotypes, ethylene and/or jasmonic dependent pathways are activated (Fig. 3), but they would be inefficient in fighting against *T. deformans*.

The production of so-called pathogenesis-related (PR) proteins (van Loon *et al.* 2006) is another inducible defense mechanism that is activated in *P. persica* upon *T. deformans* attack, as evidenced by the up regulation of *PpPR10* and *PpTLP-1* (Fig. 3) in both susceptible and resistant genotypes. Members of the PR 10 family are known as peach major allergens (Pru p 1.01 and Pru p 1.06D) and have also been related to decreased susceptibility to *Monilinia* spp. during stone hardening (Zubini *et al.* 2009). On the other hand, TLPs are β-1,3-glucanases belonging to the PR 5 protein family. In leaves of *P. persica, PpTLP-1* and *-2* were considerably more highly expressed in a cultivar resistant to *Xanthomonas campestris* pv. *pruni* than in a susceptible one in response to bacteria inoculation (Sherif *et al.* 2012). In the case of fruits of *Prunus domestica* challenged with the fungus *M. fructicola,* while the levels of *PdPR5-1* are constitutively higher in the resistant genotypes, the transcript levels promptly increased during the first days after infection (El-kereamy *et al.* 2011). The induction of *PpPR10* and *PpTLP-1* in both resistant and susceptible genotypes is indicative of their participation in an early response of *P. persica* which is not sufficient to confer resistance against pathogens. The up-regulation of these PR proteins in susceptible plants, together with other components of the basal plant defense machinery described before, also indicates that the host is recognizing *T. deformans* most probably through the so-called pathogen-associated molecular patterns like β-glucans by pattern recognition receptors (Macho & Zipfel 2006). By contrast, *PpDfn1* which was differentially induced in the resistant genotype, has been previously cloned and it was demonstrated that the product of this gene inhibits the germination of various fungal pathogens (Wisniewski *et al.* 2003). Similarly, PpDfn1 may have functional activity against *T. deformans.* Thus, the lack of induction of *PpDfn1* correlates with *P. persica* susceptibility to the fungus.

Time course evaluation of PR proteins may also provide information concerning mechanisms operating in the pathogen. *Ustilago maydis*, one of the most studied biotrophic fungi infecting maize, suppresses early maize response genes after initial activation (Doehlemann *et al.* 2009). On the other hand, the hemibiotrophic fungus *Colletotricum graminicola* does not offset host defenses during the biotrophic phase (Vargas *et al.* 2012). Here, a non-uniform response was observed, with a more pronounced tendency of defense repression in the susceptible genotypes. On one hand, *PpLTP1* is dramatically reduced upon pathogen infection in the three genotypes (Fig. 3), while other PR genes are depressed only in susceptible genotypes (i.e. *PpDfn*1 in DS and FL) and a further group show early peaks of induction followed by restoration of normal levels of transcripts (i.e. *PpPAL1* in susceptible genotypes). Once again, these results highlight the particularities of the pathosystem under study.

Some metabolites related to plant defense, such as Pro (Szabados *et al.* 2009), chlorogenic acid (Fuchs & Spiteller, 1998) and spermidine (Walters *et al.* 2003) were also induced in all genotypes in early and/or later phases (Fig. 5 and 7) after inoculation; nevertheless, their induction seems to be insufficient to confer resistance to the disease since they are also induced in susceptible genotypes. It is interesting to note, that while increases in *PpP5CS1* in DS and also of *Ppδ OAT* in DR may explain the early rise in Pro content when facing the yeast form of the fungus (Fig. 8), the increase of this amino acid in FL may be controlled by other enzyme such as proline dehydrogenase (Qamar *et al.* 2015). Moreover, a second peak of Pro was detected in DR at 72 hpi when the filamentous form of *T. deformans* is detected. In this case, this peak parallels with that of *PpP5CS2* and could have an impact in the defense responses against *T. deformans* (Fig. 8 and 9). In Arabidopsis, different genes involved in Pro metabolism are induced depending of the type of interaction (virulent,

avirulent or non-host pathogen infection), with the *AtP5CS2* gene mediating P5C and Pro contents under Avr-R and non-host interactions (Qamar *et al.* 2015).

The early peak of carotenoid induction in the three genotypes and of anthocyanins in DR and FL (Fig. 4) may contribute to the general defense process in *P. persica.* Carotenoids provide high antioxidant activities and as such are effective in dealing with pathogen induced ROS production. Anthocyanins have also been related to plant defense (Schaefer *et al.* 2008). In this respect, the general decrease in total phenolics during the first 24 hpi is rather surprising. The following increase in phenolics, could contribute to the defense, as accounted by increases in flavonoids, benzoic acid and chlorogenic acid as well (Fig. 4 and 5).

The analysis of total phenolics, flavonoids and *PpPAL1* performed here, indicates that secondary metabolites are important elements in the defense responses against *T. deformans*. Future studies will be focused on the analysis of particular secondary metabolites induced in *P. persica* when challenged with the fungus, and in the elucidation of their role in this interaction.

Metabolomics of *P. persica* leaves reveals biphasic responses upon *T. deformans* inoculation and different profiles in the resistant and susceptible genotypes

Metabolic profiling of *P. persica* leaves revealed common and distinct responses to *T. deformans* in susceptible and resistant genotypes. Metabolomics also disclosed biphasic responses in all cases a fact that is likely corresponding to the presence of either of the two forms of the fungus, the inoculated yeast form and the later mycelial development (Fig. 1). PCA analysis (Fig. 4) depicts a clear separation, based on their metabolic profiles, between the resistant and the susceptible genotypes challenged with *T. deformans* for a period of 120 h. These results on one hand denote differential host modulation of primary and intermediary

metabolism to halt fungal spread and on the other hand differential fungal load that perturbs plant metabolism to different extent, depending on the genotype.

In susceptible genotypes, the similar magnitude of increase in Glu, Asp, and its derivative Thr, accompanied by increases in other amino acids derived from pyruvate (Ile, Val and Ala) and glycerate (Ser) in pathogen-challenged leaves, suggests these amino acids might function as N resource for the growing pathogen. Increases in these amino acids have similarly been described in other pathosystems involving biotrophic fungi. The patterns of Met, Arg, Trp, Tyr, Phe, Pro and Orn accumulation are a general feature of pathogenesis (Parker *et al.* 2009); nevertheless, they could also be used as N source for the pathogen. *T. deformans* encodes several putative amino acids transporters (TAPDE_002618g.01, TAPDE_003704g.01, TAPDE_000578g.01; TAPDE_002447g.01, TAPDE_002941g.01, TAPDE_003537g.01) that may allow the up-take of these amino acids. In other pathogenic fungi such as *U. maydis* (Lanver *et al.* 2014); *Magnaporthe oryzae* (Oh *et al*. 2008) and *Uromyces fabae* (Struck *et al.* 2004), the fungal up-regulation of transporters that enable nutrient uptake (amino acid and peptide transporters) has been observed during the biotrophic phase. Therefore, amino acids and peptides are likely to be nutrients for fungal growth and development during the early stages of colonization.

The increased amounts of glucose, can not only serve as a source of energy, but also as a carbon source for fungal cell wall building since this sugar is the main component of the cell wall of the yeast form of *T. deformans* (Petit & Schneider, 1983). Galactose and rhamnose are additional components of fungal cell wall and they also increase upon infection (Fig. 5 and 7). Other metabolites, such as the sugars sucrose and fructose, the alcohol glycerol and the organic acid malate (12 hpi), that also may support yeast growth also rise early after inoculation (Fonseca & Rodriguez, 2011). In this respect, in *U. maydis* the induction of a high affinity sucrose transporter during filament and appressorium formation is a key

virulence factor required for biotrophic growth (Whal *et al.* 2010; Lanver *et al.* 2014). These results are consistent with a biotrophic behavior in which *T. deformans* establishes a dynamic relationship with host cells that provide the nutrients to maintain the fungal development and reproduction. Some clues regarding *T. deformans* adaptation to its host *P. persica*, can be found analyzing the fungus genome; as genes involved in plant cell wall hydrolysis (cellulase, xylanase, cutinases and other proteases), secondary metabolism, glyoxylate cycle, detoxification, sterol biosynthesis, can all be detected. In addition, its genome encodes most of the enzymes involved in primary metabolism (citric acid, glycolysis, biosynthesis of amino acids, lipid metabolism) and response to oxidative stress as well as key factors to ensure invasion and proliferation in plant tissue (Cissé *et al.* 2013).

Asn is conspicuously increased largely than the other amino acids (Fig. 5 and 7). Asn may have different roles in the pathogenesis: (a) it could act as a nitrogen source for the yeast form of the fungus since increases only when the yeast is present. In addition to amino acids transporters, *T. deformans* genome also harbors an Asparaginase (TAPDE_002171g.01) to metabolize Asn. In fact, it is reported that this species assimilates Asn (Moore 2011); (b) it may induce *T. deformans* dimorphism, as it is the case of *Aureobasidium pullulans* for which Asn has been demonstrated to have a direct influence in the yeast-mycelium dimorphism (Park 1982); (c) Asn may activate pathogenesis related genes. Studying the pathosystem *Pisum sativum* - *Nectria haematococca,* Yang and colleagues (2005) proposed this amino acid as inductor of the expression of a fungal virulence gene (*pel*D) that allows fungal proliferation and development. Here in the case of *P. persica*-*T. deformans*, the increase in Asn relative levels also seem to be related to fungal pathogenesis since Asn does not increase in the resistant genotype (DR). It remains to be elucidated whether this amino acid triggers *T. deformans* dimorphism and/or pathogenesis.

Another metabolite that warrants attention is Trp, which in both susceptible plants (DS and FL) exhibits two peaks of induction (Fig. 5 and 7). Trp is the precursor for the synthesis of the hormone auxin, phytoalexins and indole alkaloids. The symptoms of the disease (hyperplasia and tissue curling) have been related to a leaf hormonal imbalance caused by the fungus. Consistent with increased levels of IAA in infected tissue (Raggi 1995) are the greater levels of Trp that could support the induced synthesis of auxins during pre-symptomatic stages of the disease. In this respect, the analysis of *T. deformans* genome allowed the identification of the genes *Tam* and *Iad* encoding putative Trp aminotransferase and indole-3-acetaldehyde dehydrogenase, respectively, which at least in *Ustilago maydis* are involved in IAA biosynthesis (Cissé *et al.* 2013). Thus, *T. deformans* appears to manipulate plant cell metabolism in susceptible genotypes to support increased IAA synthesis. It is not clear yet, however, whether the source of IAA is the host cell, the fungus or both.

Ornithine is a precursor of polyamine biosynthesis in the reaction catalyzed by ornithine decarboxylase (ODC) which converts it to putrescine. In various dimorphic fungi, such as *U. maydis* (Guevara-Olvera *et al.* 1997) and *Yarrowia lipolytica* (Jiménez-Bremont *et al.* 2001), levels of putrescine higher than those necessary to sustain vegetative growth are required for the dimorphic transition; and transition to the mycelial form depends on the fungal ODC activity. The *T. deformans* genome sequence revealed the presence of a gene encoding ODC (TAPDE_002031g.01). The Orn profile (Fig. 7) could be explained in terms of a yeast Orn demand by ODC to synthetize putrescine that leads to a net early decrease in the free amino acid in the leaf. The same Orn variation pattern was observed in both resistant and susceptible genotypes, in agreement with transition to the filamentous form in all cases (Fig. 1).

It is additionally worth discussing that raffinose, and its precursor galactinol, distinctively accumulated in a concerted manner in susceptible plants upon *T. deformans* inoculation (Fig. 5 and 7). Galactinol and raffinose have been postulated to protect plant tissues from abiotic stresses (Nishizawa *et al.* 2008) while raffinose has additionally been proposed to function as a signaling molecule (ElSayed *et al.* 2013). Moreover, a role of these compounds in biotic interactions is starting to emerge; i.e. galactinol has been suggested as a signaling component of the Induced Systemic Resistance in cucumber plants (Kim *et al.* 2008). Nevertheless, in the case of *P. persica-T. deformans* interaction, if the role of raffinose were to be involved in defense mechanisms it would be expected to also increase in the resistant genotype upon fungal inoculation. Another possibility is that raffinose serves as substrate for *T. deformans* development. Although it has been reported that *T. deformans* does not use raffinose as substrate for growth (Fonseca & Rodriguez, 2011), other species with the genus *Taphrina* do. In addition, the *T. deformans* genome encodes for a gene involved in raffinose catabolism (TAPDE_002196g.01 (http://genome.jgi.doe.gov/pages/search-for-genes.jsf?organism=Tapde1_1), CCG82303.1 http://www.ebi.ac.uk/ena/data/view/CCG82303 encoding a putative SIP2). In addition, no sequences for genes involved in raffinose synthesis were found in *T. deformans* genome. Considering that *T. deformans* is a dimorphic fungus and that *in vitro* experiments are conducted with the yeast form, the possibility that *T. deformans* uses raffinose when infecting host tissue and/or when changing to its filamentous form cannot be excluded. In fact, nothing is known concerning substrate utilization and carbon source sequestration by the *T. deformans* when growing in *P. persica* leaves. Thus, the increase in raffinose could be an indicator that plant metabolism has been manipulated by the fungus. The absence of genes encoding Raffinose Synthase (RS) in the fungus genome indicates that the increase in raffinose detected in susceptible leaves upon infection is due to a host synthesis and not due

to the pathogen. In addition, other interesting points to highlight are the differences in gene expression among genotypes. In the susceptible genotype FL, increased levels of raffinose seem to be related to the significant decrease in *PpSIP2* involved in raffinose catabolism (Fig. 8). Previously, it has been reported that in heat-treated peach fruit the levels of transcripts of the catabolizing enzyme correlates with raffinose accumulation (Lauxmann *et al.* 2014). On the other hand, in the susceptible genotype DS, raffinose accumulation seem to be related to expression of both *PpRS* (its increase at 12 hpi precedes raffinose peak at 24 hpi) and *PpSIP1-2* which are induced at 72-96 hpi when raffinose decreases (Fig. 8). In this respect, accumulation of transcripts encoding RS have been previously shown to correlate with an increase in raffinose (Saito & Yoshida 2012; Egert *et al.* 2013). These differences in the responses among genotypes also reinforce the hypothesis that synthesis of raffinose is not part of a defense strategy of *P. persica.*

Taken together, in inoculated susceptible leaves the biphasic lifestyle of the fungus and the wave-ish modifications in both metabolites and in the defenses mechanisms, fit into the following model. Peaks of increases of many amino acids, organic acids and sugars precede or overlap with the first maximum of *T. deformans* when it is present in its yeast form. Therefore, these metabolites might function as nutrients to feed the fungi. The yeast form induces non-host biochemical changes as callose deposition and HR. In addition, early increases in *PpTLP1, PpPAL1, PpPR10,* anthocyanins, carotenoids, chlorogenic acid and benzoate, among others, accompany this process. At this stage, Asn may activate pathogenesis related genes in *T. deformans* whose effects may be appreciated later. After 48 hpi *T. deformans* turns into its filamentous form. Even though this is the parasitic from of the fungi, during the transition to the hyphae and early after, *T. deformans* may be more susceptible to plant defenses (PpDfn1, PpPR10, total phenolics, flavonoids) as accounted for a decrease in the quantification of *T. deformans* at 72 hpi. After that, fungal load rises again,

accompanied with smaller increases in amino acids and organic acids, which turned to reestablish the plant homoeostasis to set up of biotrophic lifestyle. At this stage, the secretion of lytic enzymes by the pathogen alters the interface fungus-leaf cell wall allowing the fungal growth. Future studies should encompass the effector proteins expressed by the fungal cells which contribute to fungal pathogenesis and which are not known at present.

Differential features occurring in the resistant genotype when challenged with *T. deformans*

Although it has been reported that resistance to *T. deformans* is a polygenic trait (Padula *et al*. 2008) little is known about *P. persica–T. deformans* interactions at the molecular and biochemical levels and no information is available regarding the mechanisms involved in the resistance. Confocal microscopy examination of *P. persica* leaves inoculated with *T. deformans* in its yeast phase revealed fungal dimorphism, regardless of the plant genotype (Fig. 1). Thus, the resistance to *T. deformans* can be attributed to molecular and biochemical mechanisms that restrain further hyphae proliferation and/or the development of the disease and not to fungal dimorphism avoidance.

One layer of defense that pathogens face is the production of compounds with anti-pathogenic properties such as phenolic compounds and reactive oxygen species (Heller & Tudzynski, 2011). In this respect, DR displays an earlier induction of superoxide production than susceptible genotypes (Supporting Information Fig. S2). In addition, DR plants present higher levels of flavonoids than FL and DS, before and after being challenged with *T. deformans* (Fig. 4). In addition, DR is the only genotype that exhibits a net increase in total phenolics with respect to 0 hpi. This peak at 96 hpi matches with that of flavonoids at 96 hpi, indicating that flavonoids are, at least, contributing to the increase in total phenolics

accumulation (Fig. 4). Moreover, *PpPAL1* transcript accumulation occurs at 72 hpi in DR and precedes the rise in flavonoids (Fig. 3). In concordance with these results, higher levels of phenolic compounds were measured in leaves of a tolerant advanced peach tree selection in comparison with very susceptible trees (Padula, 2010). Here, the fact that *T. deformans* charge diminishes at 96 hpi, after reaching maximum levels at 72 hpi (Fig. 2), certainly denotes the participation of these compounds in the defense against *T. deformans* and it could account, at least in part, for the resistance to the disease. It remains to be elucidated whether the increase in flavonoids is due to enhanced synthesis of the same pre-existing flavonoids or due to the induced synthesis of a different type.

Another differential response is the exclusive up-regulation of *PpICS* in DR (Fig. 3). Interestingly, up-regulation of *PpDfn1* at 48 hpi (Fig. 3) in DR when hyphae start development in the inoculated tissue (Fig. 1) and of *PpPAL1* are independent of SA pathway since their increase occurs before the rise in *PpICS* (Fig. 3). SA is thought to be essential for inducing resistance against biotrophic pathogens (Glazebrook 2005) and this would be the case for DR genotype. For comparison, in other pathosystem, the infection of susceptible maize with *U. maydis*, which conducts to the development of the typical disease tumors, was not accompanied by a significant induction of SA-dependent pathways; as one of its markers PR1 was not detected early after infections and poorly detected later on (Doehlemann *et al.* 2008). SA treatment of the host plant before *U. maydis* inoculation prevents the proliferation of the fungus (Djamei *et al.* 2011). Moreover, *U. maydis* possess a salicylate hydroxylase which is up-regulated during its biotrophic stages and that could decrease the SA content (Rabe *et al.* 2013).

In addition, xylose makes a significant contribution to PC1 (Fig. 6, Supporting Information Table S2) and exhibits a differential behavior in DR than in the susceptible genotypes (Fig. 5 and 7). Variations in the quantity of xylose in the cell wall have been related to resistance/susceptibility to pathogens (Sánchez-Rodríguez *et al.* 2009). In plants, xylose is a central constituent of hemicellulose in the cell wall, which is incorporated to this fraction as UDP-Xyl synthesized from UDP-Glc (Harper & Bar-Peled, 2002). Therefore, increased free xylose in DR upon inoculation is not indicative of exacerbated cell wall biosynthesis. Nevertheless, it would be interesting to analyze the cell wall composition in the different genotypes to seek for differences. Most of the data presented shows that upon pathogen *T. deformans* inoculation, the shikimic acid pathway is activated in both resistant and susceptible genotypes (Fig. 9). Shikimate is the precursor of Phe, Tyr, Trp, auxins, SA, lignin, flavonoids and other phenylpropanoids. Chorismate is a central node in the synthesis of aromatic amino acids and secondary metabolites. On one hand the phenylpropanoid route is induced in all genotypes, as accounted by increases in relative accumulation of *PpPAL1* and some of the following compounds; Phe, Tyr, total phenolics, flavonoids, chlorogenic acid (Fig. 4, 5 and 7). On the other hand, chorismate may follow divergent branches. While the SA production is activated in the resistant genotype (DR), accounted for by rises in *PpICS* (Fig. 3), the indole pathway is up-regulated in the susceptible genotypes as supported by the dramatic increase in Trp in FL and DS. Therefore, while induction of SA may conduct to activation of a cascade of defense responses in DR, the induction of the indol pathway in susceptible plants may support auxin biosynthesis in the infected tissue leading to the development of hypertrophy and hyperplasia, both symptoms of the disease (Fig. 9). In this respect, an interesting point to highlight is that SA was identified as a repressor of auxin signaling (Wang *et al.* 2007); thus, any increase in SA in DR would also contribute to the

prevention of hyperplasia development. Therefore, in future studies it would be of interest the elucidation of the responses triggered by SA in *P. persica*.

CONCLUSION

This is the first time that early events in the *T. deformans-P. persica* interaction are characterized and that fungal dimorphism is achieved under laboratory conditions. On one hand, our results reveal a biphasic re-programming of plant tissue in susceptible genotypes, with a first stage to provide metabolites that allow the reproduction of the yeast phase and the second, the development of the hyphae. On the other hand, the presence of different responses such as ROS, cell death, callose deposition, induction of proline and chlorogenic acid accumulation are observed independently of the genotype analyzed. Regarding the tolerant genotype, *P. persica*, resistance to *T. deformans* appears to be regulated by a complex defense network involving SA and a set of defense proteins (i.e. PpDFN1) and metabolites. Knowledge obtained here will help in the engineering of strategies to develop novel resistant genotypes to be used in breeding programs. Availability of tolerant cultivars is important not only for the economy but also for the environment since a reduction of the considerable amounts of fungicides currently used to control this pathogen could be achieved.

CONFLICT OF INTEREST

The authors have no conflicts of interest to declare.

ACKNOWLEDGMENTS

L.A.S, C.A.B, M.F.D, G.L.M. and M.V.L. are members of the Researcher Career of CONICET. C.A.B. was recipient of a fellowship from Alexander von Humboldt Foundation at A.R.F. We thank Professor Dr. E. Bellini and Dr. E. Giordani (Dipartimento di Scienze Produzioni Agroalimentari e dell'Ambiente (DISPAA), Universita di Firenze) for providing

P. persica selections DOFI-84.364.089 and DOFI-84.364.060. This work was supported by Agencia Nacional de Promoción de Actividades Científicas y Técnicas (PICT 2012-1376). INTA supported the *P. persica* collection at EEA San Pedro (PNFRU 1105062; REDGEN 1137021; PReT 127128).

References

Bari R. & Jones J.D. (2009) Role of plant hormones in plant defense responses. *Plant Molecular Biology* **69,** 473–488

Bassi M., Conti G. & Barbieri N. (1984) Cell wall degradation by *Taphrina deformans* in host leaf cells. *Mycopathologia* **88,** 115-125

Bellini E., Giordani E., Perria R. & Paffetti D. (2002) Leaf Curl in Peach: new resistant genotypes and molecular markers. *Acta Horticulturae* **592**, 649-653

Cantín C.M., Moreno M.A. & Gogorcena Y. (2009) Evaluation of the Antioxidant Capacity. *Journal of Agricultural Food Chemistry* **57,** 4586–4592

Chen X.-Y. & Kim J.-Y. (2009) Callose synthesis in higher plants. *Plant Signaling & Behavior* **4,** 489–492

Cissé O.H., Almeida J.M.G.C.F., Fonseca A., Kumar A.A., Salojärvi J., Overmyer K., Hauser P.M. & Pagni M. (2013) Genome sequencing of the Plant Pathogen *Taphrina deformans*, the Causal Agent of Peach Leaf Curl. *MBio* 4: e00055-13

Çmen I.´ & Ertugrul B.B. (2007) Determination of Mycoflora in Almond Plantations Under Drought Conditions in Southeastern Anatolia Project Region, Turkey. *Plant Pathology Journal* **6,** 82-86

Dean R., Van Kan J.A.L., Pretorius Z.A. , Hammond-Kosack K.E. , Di Pietros A., Spanu P.D., Rudd J.J., Dickman M., Kahmann R., ELLIS J. & Foster G.D. (2012) The Top 10 fungal pathogens in molecular plant pathology. *Molecular Plant Pathology* **13,** 414–430

De Vleesschauwer D., Gheysen G. & Hofte M. (2013) Hormone defense networking in rice: tales from a different world. *Trends in Plant Science* **18,** 555–565

Doehlemann G., Wahl R., Horst R.J., Voll L.M., Usadel B., Poree F., Stitt M., (…) Kämper J. (2008) Reprogramming a maize plant: transcriptional and metabolic changes induced by the fungal biotroph *Ustilago maydis*. *Plant Journal* **56,** 181–195

Egert A., Keller F. & Peters S. (2013) Abiotic stress-induced accumulation of raffinose in Arabidopsis leaves is mediated by a single raffinose synthase (*RS5*, At5g40390). *BMC Plant Biology* **13,** 218

El-kereamy A., El-sharkawy I., Ramamoorthy R., Taheri A., Errampalli D., Kumar P. & Jayasankar S. (2011) *Prunus domestica* Pathogenesis-Related Protein-5 activates the defense response pathway and enhances the resistance to fungal infection. *PLoS One* **6,** e17973

ElSayed A.I., Rafudeen M.S. & Golldack D. (2013) Physiological aspects of raffinose family oligosaccharides in plants: protection against abiotic stress. *Plant Biology* **16,** 1-8

Ferreira R.B., Monteiro S., Freitas R., Santos C.N., Chen Z., Batista L.M., Duarte J., Borges E., Teixeira A.R. (2007) The role of plant defence proteins in fungal pathogenesis. *Molecular Plant Pathology* **8,** 667-700

Fuchs C.T. & Spiteller G. (1998) Accumulation of Caffeoyl-D-quinic Acids and Catechins in plums affected by the fungus *Taphrina pruni*. *Z Naturforsc* **53c,** 799-805

Glazebrook J. (2005) Contrasting Mechanisms of Defense Against Biotrophic and Necrotrophic Pathogens. *Annual Reviews in Phytopathology* **43,** 205-227

Gohari A.M., Ware S.B., Wittenberg A.H.J., Mehrabi R., M'Barek S.B., Verstappen E.C.P., van der Lee T.A.J., Robert O., Schouten H.J., de Wit P.P.J.G.M. & Kema G.H.J. (2015) Effector discovery in the fungal wheat pathogen *Zymoseptoria tritici. Molecular Plant Pathology* **16,** 931-945

Guevara-Olvera L., Xoconostle-Cázares B. & Ruiz-Herrera J. (1997) Cloning and disruption of the ornithine decarboxylase gene of *Ustilago maydis*: evidence for a role of polyamines in its dimorphic transition. *Microbiology* **143,** 2237-2245

Harper A.D. & Bar-Peled M. (2002) Biosynthesis of UDP-Xylose. Cloning and Characterization of a Novel Arabidopsis Gene Family, *UXS*, Encoding Soluble and Putative Membrane-Bound UDP-Glucuronic Acid Decarboxylase Isoforms. *Plant Physiology* **130,** 2188-2198

Heller J. & Tudzynski P. (2011) Reactive oxygen species in phytopathogenic fungi: signaling, development, and disease. *Phytopathology* **49,** 369-90

Jiménez-Bremont J.F., Ruiz-Herrera J. & Domínguez A. (2001) Disruption of gene *Y/ODC* reveals absolute requirement of polyamines for mycelial development in *Yarrowia lipolytica*. *FEMS Yeast Research* **1,** 195-204

Kim M.S., Cho S.M., Kang E.Y., Im Y.J., Hwangbo H., Kim Y.C., Ryu C.-M., (…) & Cho B.H. (2008) Galactinol Is a Signaling Component of the Induced Systemic Resistance Caused by *Pseudomonas chlororaphis* O6 Root Colonization. *Molecular Plant-Microbe Interactions* **21**, 1643–1653

Kopka J., Schauer N., Krueger S., Birkemeyer C., Usadel B., Bergmuller E., Dormann P., (...) & Steinhauser D. (2005) GMD@CSB. DB: the golm metabolome database. *Bioinformatics* **21**, 1635–1638

Lauxmann M.A., Borsani J., Osorio S., Lombardo V.A., Budde C.O., Bustamante C.A., Monti L.L., (...) & Lara M.V. (2014) Deciphering the metabolic pathways influencing heat and cold responses during post-harvest physiology of peach fruit. *Plant Cell & Environment* **37,** 601–616

Lo Presti L, Lanver D, Schweizer G, Tanaka S, Liang L, Tollot M, Zuccaro A, Reissmann S, Kahmann R. (2015) Fungal effectors and plant susceptibility. *Annual Reviews in Plant Biology* **66,** 513-545

Macho A.P. & Zipfel C. (2006) Plant PRRS and the activation of innate immune signaling. *Molecular Cell* **54,** 263-272

Mc Donald M.C., Mc Donald B.A., Solomon P.S. & (2015) Recent advances in the *Zymospetoria tritici*-wheat interactions: insights from pathogenomics (2015) *Frontiers in Plant Science* **6,** 102

Mehrotra R.S. & Aneja K.R. (1990) Ascomycotina. In An introduction to mycology. New Age International (P) Limited, Publishers, New Delhi pp 288-289

Mix AJ (1935) The life history and cytology of *Taphrina deformans*. *Phytopathology* 25: 41-66

Moore R.T. (2011) Lalaria R.T. More. In The yeasts: a taxonomic study. Fifth edition. Eds Kurtzman C., Fell J.W. & Boekhout T. Elsevier, pp 582-591

Müller G.L., Drincovich M.F., Andreo C.S. & Lara M.V. (2010) Role of photosynthesis and analysis of key enzymes involved in primary metabolism throughout the lifespan of the tobacco flower. *Journal of Experimental Botany* **61,** 3675–3688

Nadal M., García-Pedrajas M.D. & Gold S.E. (2008) Dimorphism in fungal plant pathogens. *FEMS Microbiology Letters* **284,** 127-134

Nishizawa A., Yabuta Y. & Shigeoka S. (2008) Galactinol and raffinose constitute a novel function to protect plants from oxidative damage. *Plant Physiology* **147,**1251–1263

Padula G., Bellini E., Giordani E. & Ferri A. (2008) Further investigations on the resistance to leaf curl (*Taphrina deformans* Berk. Tul.) of peach cultivars and F1 progenies. *In* C Di Vaio, C Damiano, C Fideghelli, eds, Atti del VI Convegno Nazionale Sulla Peschicoltura Meridionale, Imago Media Editrice, Dragoni, pp 113-119

Petit M. & Schneider A. (1983) Chemical analysis of the wall of the yeast from of *Taphrina deformans*. *Achieves in Microbiology* **13,** 141-146

Pscheidt J.W. (1995) Leaf Curl. *In* JM Ogawa, EI Zehr, GW Bird, DF Ritchie, K Uriu, JK Uyemoto, eds, Compendium of stone fruits diseases, APS Press, St. Paul., USA, pp 19-20

Qamar A., Mysore K.S. & Senthil-Kumar M. (2015) Role of proline and pyrroline-5-carboxylate metabolism in plant defense against invading pathogens. *Frontiers in Plant Science* **6,** 503

Park D (1982) Amino acid nutrition and yeast-mycelial dimorphism *in Aureobasidium pullulans. Transactions of the British Mycological Society* **79**, 170-172

Parker D., Beckmann M., Zubair H., Enot D.P., Caracuel-Rios Z., Overy D.P., Snowdon S., (…) & Draper J. (2009) Metabolomic analysis reveals a common pattern of metabolic re-programming during invasion of three host plant species by *Magnaporthe grisea. Plant Journal* **59,** 723–737

Rabe F., Ajami-Rashidi Z., Doehlemann G., Kahmann R. & Djamei A. (2013) Degradation of the plant defence hormone salicylic acid by the biotrophic fungus *Ustilago maydis. Molecular Microbiology* **89,** 179-188

Rodrigues M.G. & Fonseca A. (2003) Molecular systematics of the dimorphic ascomycete genus Taphrina. *International Journal of Systematic and Evolutionary Microbiology* **53,** 607–616

Roessner-Tunali U., Hegemann B., Lytovchenko A., Carrari F., Bruedigam C., Granot D. & Fernie A.R. (2003) Metabolic profiling of transgenic tomato plants overexpressing hexokinase reveals that the influence of hexose phosphorylation diminishes during fruit development. *Plant Physiology* **133,** 84–99

Rossi V., Bolognesi M. & Languasco L. (2007) Influence of Weather Conditions on Infection of Peach Fruit by *Taphrina deformans. Phytopathology* **97,** 1625-1633

Ruiz-Herrera J. (2012) Chapter 2: cell wall composition. *In* Fungal Cell Wall: Structure, Synthesis, and Assembly, Second Edition. CRC Press, Taylor and Francis Group, Boca Raton, FL, USA, pp 7-28

Rudd J.J. (2015) Previous bottlenecks and future solutions to dissecting the *Zymoseptoria tritici*–wheat host-pathogen interaction. *Fungal Genetics and Biology* **79**, 24–28

Saito M. & Yoshida M. (2011) Expression analysis of the gen family associated with raffinose accumulation in rice seedlings under cold stress. *Journal of Plant Physiology* 168, 2268-2271

Sánchez-Rodríguez C., Estevez J.M., Llorente F., Hernandez-Blanco C., Jorda L., Pagan I., Berrocal M., (…) Molina A. (2009) The ERECTA Receptor-Like Kinase regulates cell wall mediated resistance to pathogens in *Arabidopsis thaliana*. *Molecular Plant-Microbe Interactions* **22,** 953–963

Schaefer H.M., Rentzsch M. & Breuer M. (2008) Anthocyanins Reduce Fungal Growth in Fruits. *Natural Product Communications* **3,** 1267-1272

Sherif S., El-Sharkawya I., Paliyathb G. & Jayasankar S. (2012) Differential expression of peach ERF transcriptional activators in response to signaling molecules and inoculation with *Xanthomonas campestris pv. Pruni. Journal of Plant Physiology* **169,** 731–739.

Szabados L. & Savouré A. (2009) Proline: a multifunctional amino acid. *Trends in Plant Science* **15,** 89-97

Sziràki I., Balaàzs E. & Kiràli Z. (1975) Increased levels of cytokinin and indolacetic acid in peach leaves infected with *Taphrina deformans*. *Physiological Plant Pathology* **5,** 45-50

Tavares S., Inácio J., Fonseca A. & Oliveira C. (2004) Direct detection of *Taphrina deformans* on peach trees using molecular methods. *European Journal of Plant Pathology* **110,** 973–982

Tsai I.J., Tanaka E., Masuya H., Tanaka R., Hirola Y., Endoh R., Sahashi N. & Kikcuhi T. (2014) Comparative Genomics of *Taphrina* Fungi Causing Varying Degrees of Tumorous Deformity in Plants. *Genome Biology and Evolution* **6,**861–872

Tollot M., Assmann D., Becker C., Altmüller J., Dutheil J.Y., Wegner C.-E., Kahmann R (2016) The WOPR Protein Ros1 Is a Master Regulator of Sporogenesis and Late Effector Gene Expression in the Maize Pathogen *Ustilago maydis. PloS Pathogens* **12,** e 1005697

van Loon L.C., Rep M. & Pieterse C.M. (2006) Significance of inducible defense-related proteins in infected plants. *Annual Reviews in Phytopathology* **44,**135-62

Vargas W.A., Sanz Martín J.M., Rech G.E., Rivera L.P., Benito E.P., Díaz-Mínguez J.M., Thon M.R. & Sukno S.A. (2012) Plant Defense Mechanisms Are Activated during Biotrophic and Necrotrophic Development of *Colletotricum graminicola* in Maize. *Plant Physiol*ogy **158,** 1342–1358

Vlot A.C., Dempsey D.M.A. & Klessig D.F. (2009) Salicylic Acid, a Multifaceted Hormone to Combat Disease. *Annual Reviews in Phytopathology* **47,**177–206

Wahl R., Wippel K., Goos S., Kamper J. & Sauer N. (2010) A novel high-affinity sucrose transporter is required for virulence of the plant pathogen *Ustilago maydis*. PLoS Biol 8: e1000303

Walters D.R. (2003) Resistance to plant pathogens: possible roles for free polyamines and polyamine catabolism. *New Phytologist* **159,** 109–115

Wang D., Pajerowska-Mukhtar K., Hendrickson Culler A. & Dong X. (2007) Salicylic acid inhibits pathogen growth in plants through repression of the auxin signaling pathway. *Current Biology* **17,** 1784–1790

Yang Z., Rogers L.M., Song Y., Guo W. & Kolattukudy P.E. (2005) Homoserine and asparagine are host signals that trigger in planta expression of a pathogenesis gene in

Nectria haematococca. *Proceedings of the National Academy of Sciences of the United States of America* 11,4197-4202

Ziosi V., Bonghi C., Bregoli AM, Trainotti L., Biondi S., Sutthiwal S., Kondo S., Costa G. & Torrigiani P. (2008) Jasmonate-induced transcriptional changes suggest a negative interference with the ripening syndrome in peach fruit. *Journal of Experimental Botany* **59,** 563–573

Zubini P., Zambelli B., Musiani F., Ciurli S., Bertolini P. & Baraldi E. (2009) The RNA hydrolysis and the cytokinin binding activities of PR-10 proteins are differently performed by two isoforms of the Pru p 1 peach major allergen and are possibly functionally related. *Plant Physiology* **150,** 1235-1247

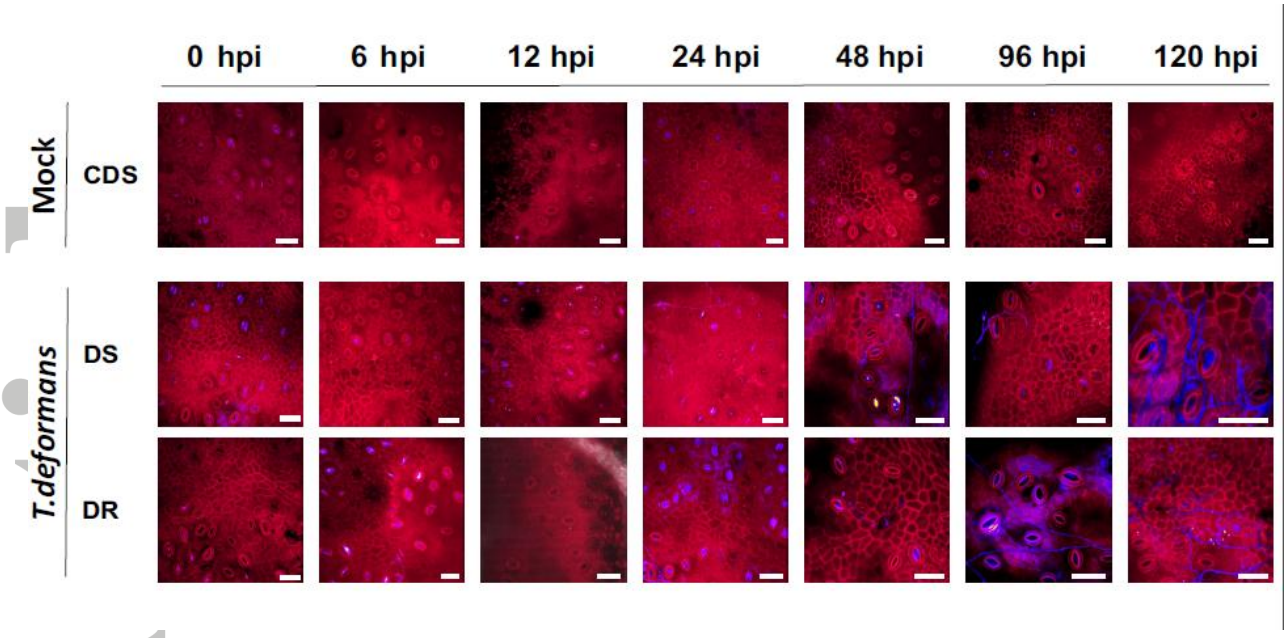

Figure 1. *P. persica* inoculation with *T. deformans* in its yeast phase. Leaves were collected after different hours post inoculation (hpi). As controls, mock-inoculated leaves of DS genotype (CDS) are shown. DS, DOFI-84.364.089; DR, DOFI-84.364.060 and FL, Flavorcrest. Abaxial side of the leaf is shown. Confocal sections of *P. persica* leaves inoculated with *T. deformans* and stained with aniline blue (fungal cell wall glucans and callose staining, blue). Autofluorescence of plant cell walls is shown in red. Bars= 50µm.

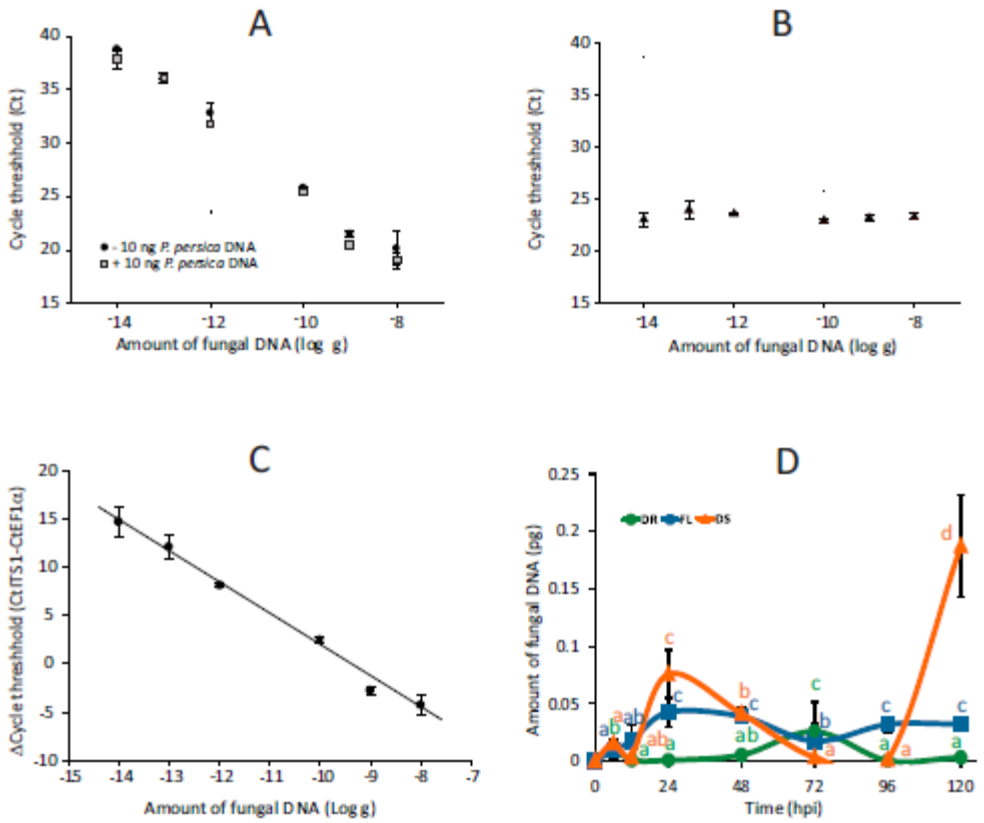

Figure 2. Quantification of *T. deformans* in leaves of different genotypes of *P. persica* after inoculation. A, Relationship between the cycle threshold (C_t) amplification of *T. deformans* ITS1 gen and total fungal DNA. Ten-fold dilutions series of fungal DNA were used to cover a range from 10 fg to 10 ng (black circles). The same curve was conducted in the presence of 10 ng of background DNA from plant (black squares). Values represent the mean of three independent determinations ± SD. B, Stability of the cycle threshold (C_t) amplification of *P. persica* EF1α gene in 10 ng of plant DNA in the presence of variable amounts of fungal DNA. Values represent the mean of three independent determinations ± SD. C, Real time PCR calibration curve. Standard curve acquired with known amounts of total DNA extracted from fungus conducted in the presence of 10 ng of plant DNA (three repetitions per concentration). D, Quantification of *T. deformans* by real time PCR amplification of ITS1 gene in leaves of resistant (DR) and susceptible (DS and FL) plants at different hours after inoculation (hpi) with the fungus in the yeast phase. The error bars represent standard

deviation of the mean (n=4). Bars with at least one same letter are not statically significant (P<0.05, Fisher test). DS, DOFI-84.364.089; DR, DOFI-84.364.060 and FL, Flavorcrest.

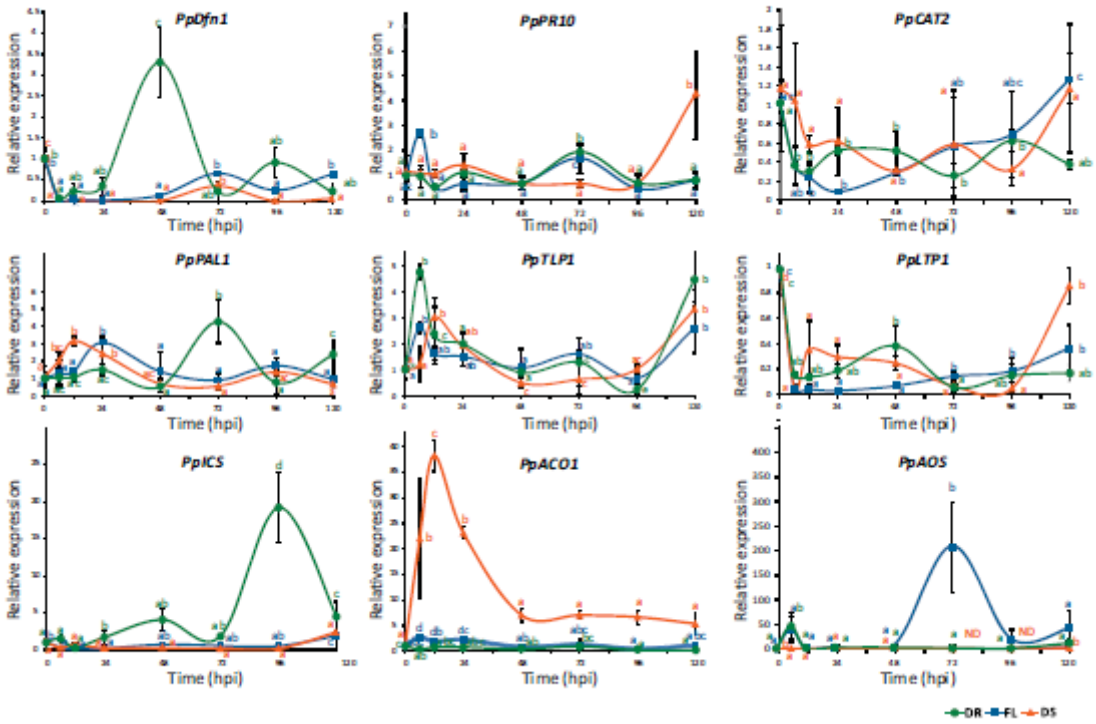

Figure 3. Expression levels of genes involved in plant defense in three different genotypes of *P. persica* inoculated with *T. deformans*. Transcript amount was assessed by quantitative real time RT-PCR, using *P. persica elongation factor 1α* (*PpEF1α*) as reference gene. Y-axes show the fold difference in a particular transcript level relative to its amount at 0 hpi in the same genotype. Values represent the mean of at least three replicates ± SD. Bars with at least one same letter are not statically significant (P<0.05). DS, DOFI-84.364.089; DR, DOFI-84.364.060 and FL, Flavorcrest inoculated with *T. deformans*.

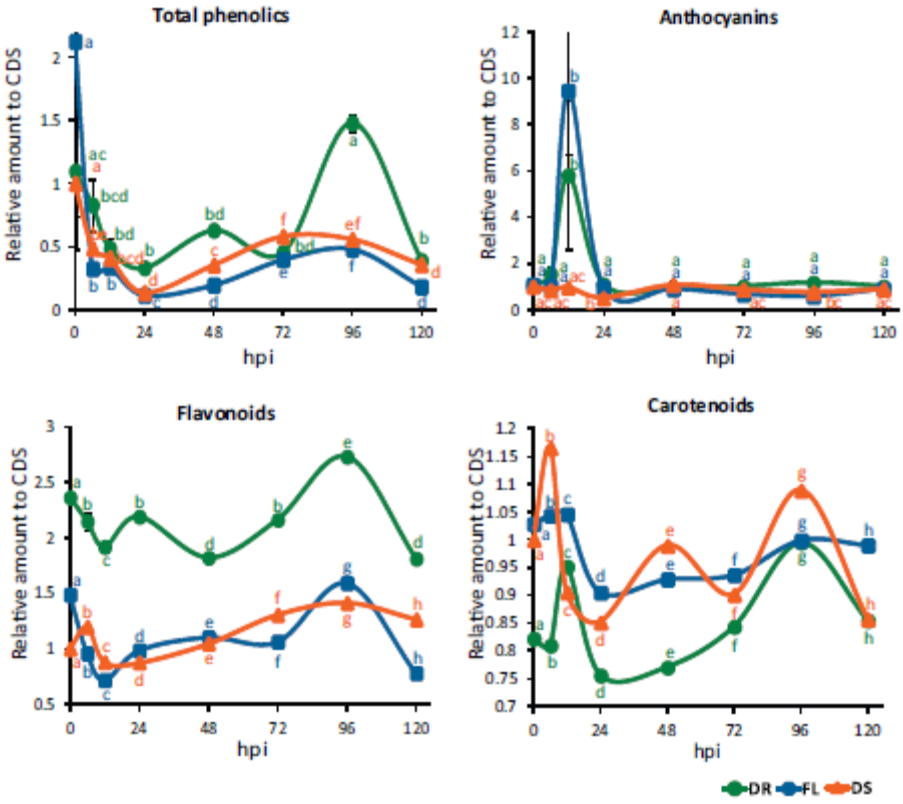

Figure 4. Changes in leaf pigments composition after inoculation. Carotenoids, flavonoids, anthocyanins and phenolics compounds are expressed in relation to the values of control DS leaves (CDS) at each time. The error bars represent standard deviation of the mean (n=3). Bars with at least one same letter are not statically significant (P<0.05). DS, DOFI-84.364.089; DR, DOFI-84.364.060 and FL, Flavorcrest inoculated with *T. deformans*.

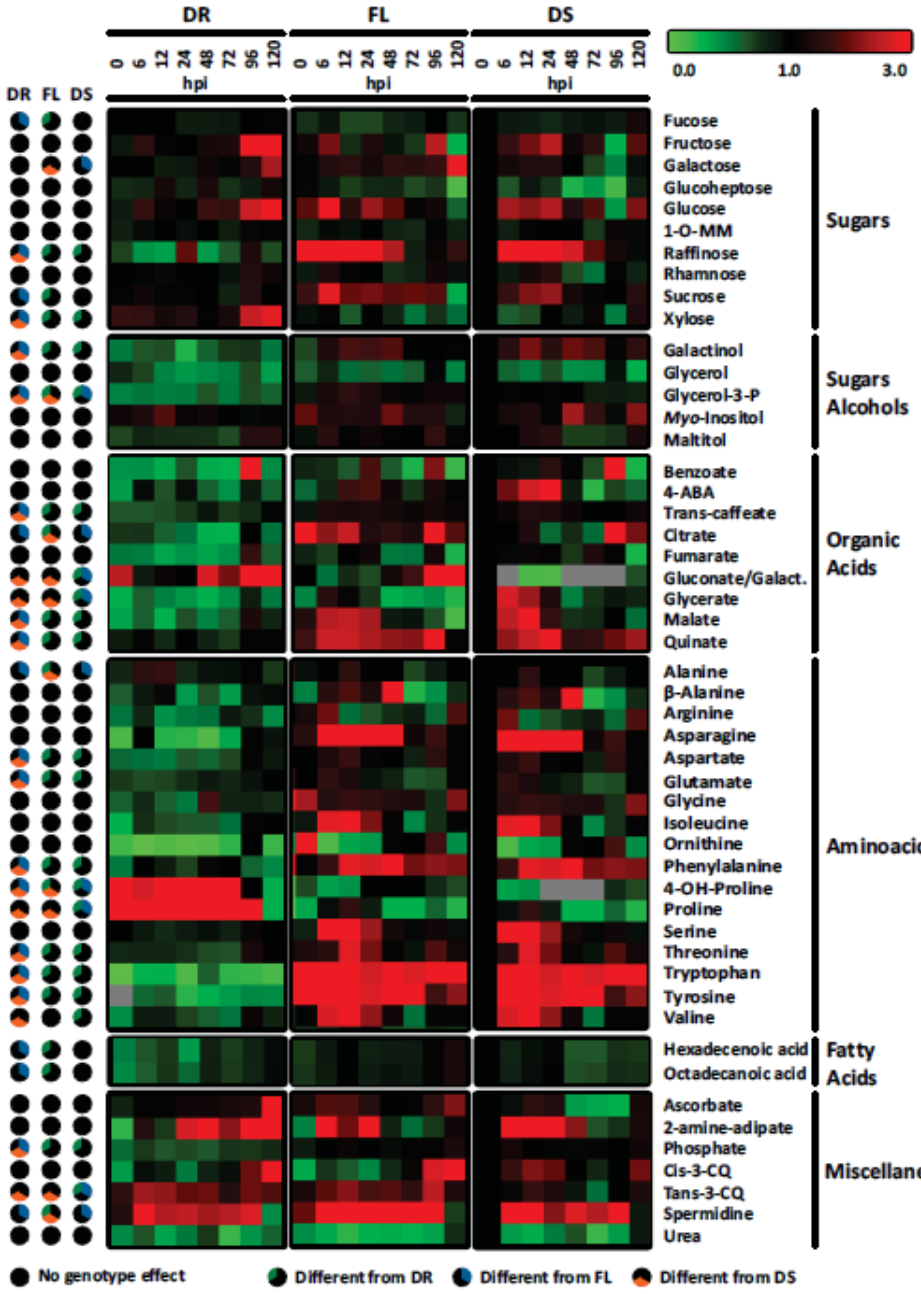

Figure 5. Metabolite profiling of *P. persica* leaves challenged with *T. deformans*. The graph shows the amounts of each metabolite in DR, DS and FL across the 120 h after inoculation with the fungus in relation to the level determined in control mock-inoculated DS leaves (CDS) at the same hpi. Normalized values are presented by using a color scale proportional to the level of each metabolite (shown at the top of the figure). Heat map was created using MeV 4.1. Relative values for each metabolite peak area are provided in Supporting

Information Table S1. Values are the mean of five biological independent determinations expressed in relation to the values in CDS at each corresponding time. Red colors and green colors indicate metabolite levels in leaves challenged with *T. deformans* greater and lower, respectively, than in the control leaves (CDS). Results from the analysis of the genotype effect on metabolite variations by two-way ANOVA are shown schematically on the left of the figure. The color of each circle indicates whether there are differences in the metabolite profile across time in the genotype indicated in the column with respect to the other genotypes tested (i.e. black stands for the absence of genotype effect; green indicates different from DR, red denotes different from DS and blue represents that the behavior differs from that of FL. DS, DOFI-84.364.089; DR, DOFI-84.364.060 and FL, Flavorcrest challenged with *T. deformans*. Cis-3-CQ, Cis-3-caffeoyl-quinic acid; 1-O-methylmannopyranoside, 1-O-MM; Trans-3-CQ, trans-3-caffeoyl-quinic acid; 4-amine-butytirate, GABA; Gluconate/Galactonate.

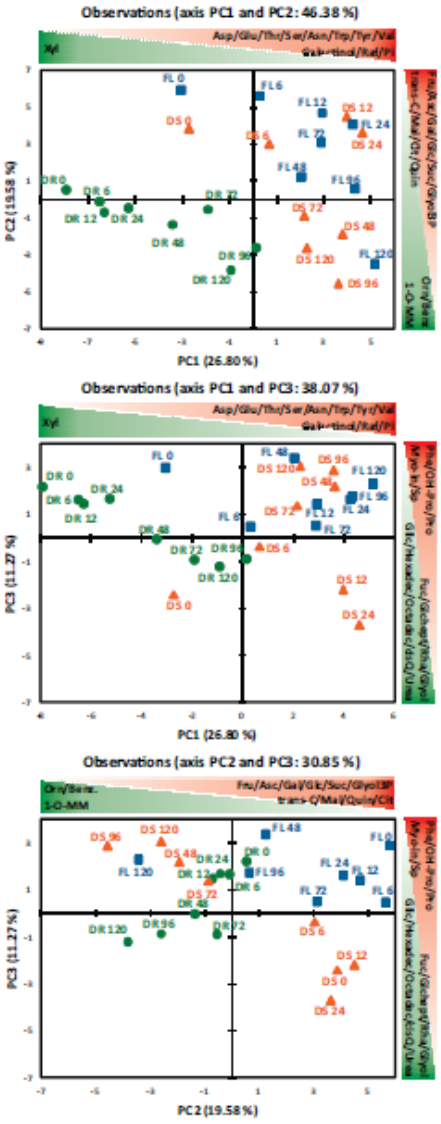

Figure 6. Principal component analysis (PCA) score plot of leaves of susceptible and resistant genotypes inoculated with *T. deformans* and analyzed by GC-MS. Variance explained by each component (%) is shown in parenthesis. Metabolites, which contribute the most to each component, are shown in red (positive contribution) and green (negative contribution). The number at the right of each name denotes the hpi of each sample; i.e. DS72 stands for DS analyzed at 72 hpi. DS, DOFI-84.364.089; DR, DOFI-84.364.060 and FL, Flavorcrest challenged with *T. deformans*. CDS, mock-inoculated control DOFI-84.364.089 leaves.

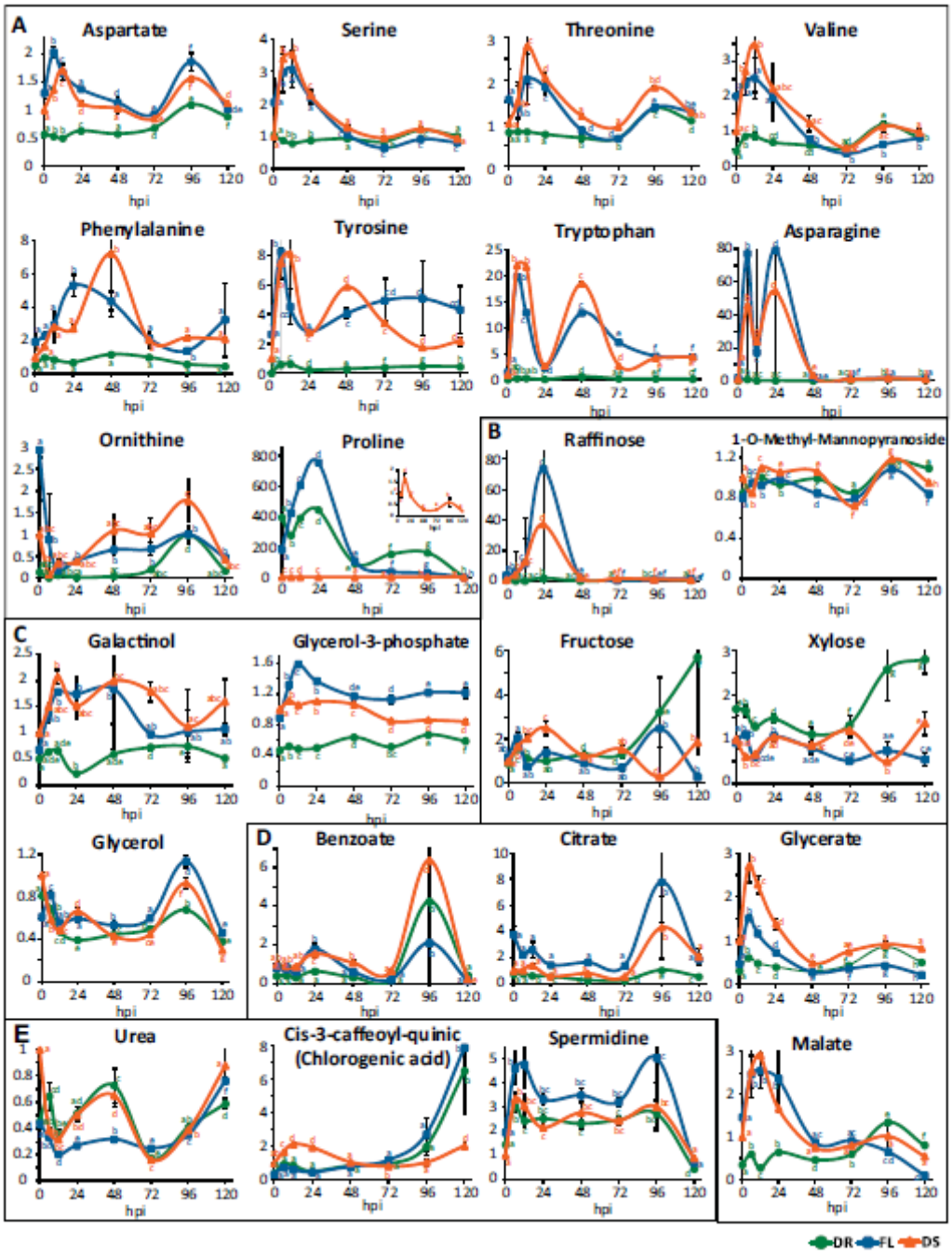

Figure 7. Metabolite concentration changes in *P. persica* leaves challenged with *T. deformans*. Graphs show the levels of each metabolite (mean of five biological independent determinations) in inoculated leaves in relation to the value (mean of five biological independent determinations) in control leaves (CDS) at the same time post-inoculation (hpi). Error bars represent standard deviation (SD). For each parameter, values with at least one same letter are not significantly different (P<0.05). Metabolites are presented by groups: A,

amino acids; B, sugars; C, sugar alcohols; D, organic acids and E, miscellaneous. DS, DOFI-84.364.089; DR, DOFI-84.364.060 and FL, Flavorcrest challenged with *T. deformans*. CDS, mock-inoculated control DOFI-84.364.089 leaves.

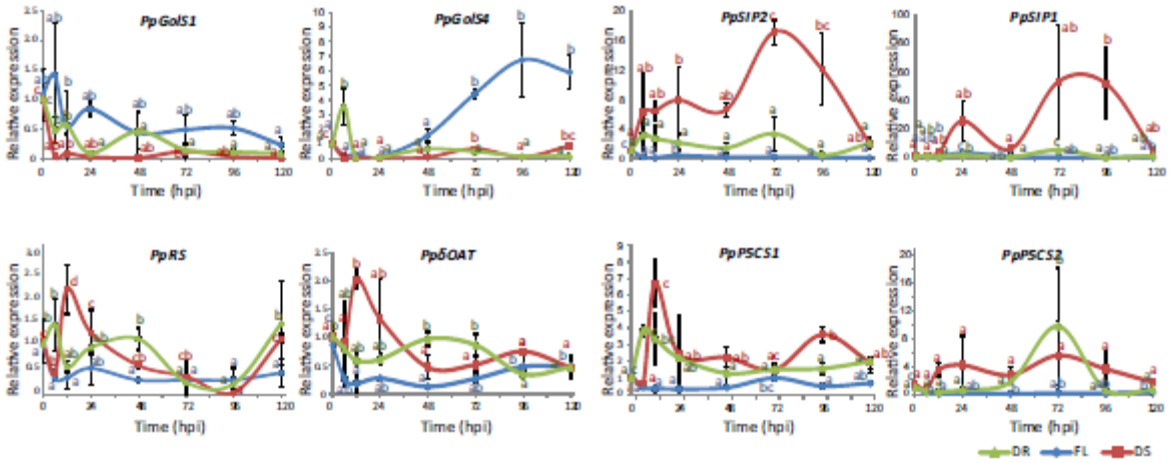

Figure 8. Expression analyses of transcripts encoding enzymes involved in raffinose (*PpGolS-1* and *-4*, *PpRS*, *PpSIP-1* and *-2*) and proline metabolism (*PpP5CS-1* and *-2*, *PpδOAT*) in *P. persica* leaves after *T. deformans* inoculation. Means (± SD) of results obtained, using three independent RNAs as template are shown. The expression level of each gene is relative to that of 0 hpi. *PpEF1α* was used as reference gene. For each transcript analyzed, bars with the same letters are not significantly different (P<0.05). DS, DOFI-84.364.089; DR, DOFI-84.364.060 and FL, Flavorcrest challenged with *T. deformans*.

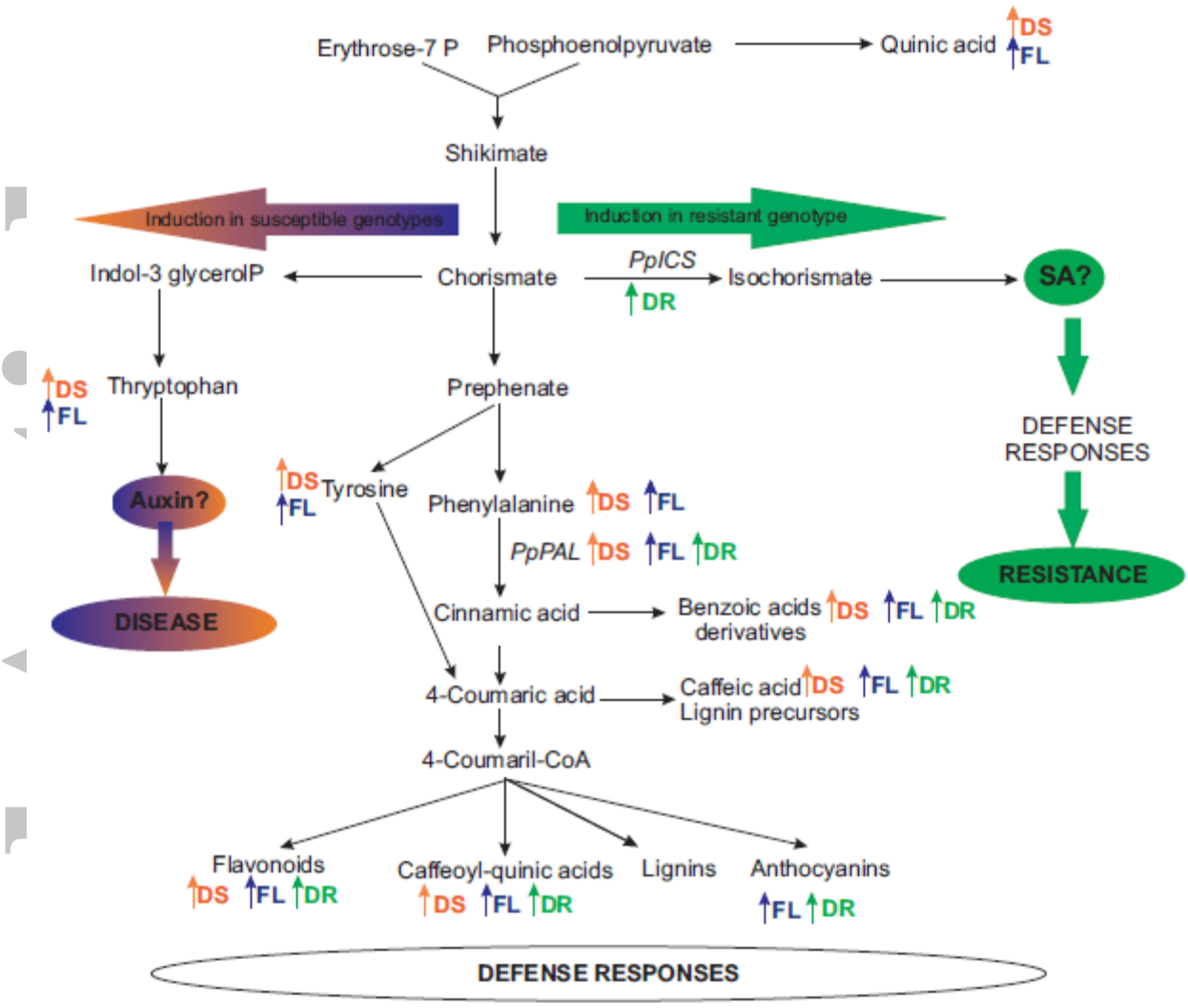

Figure 9. Schematic representation of the early response of susceptible and resistant peach genotypes to *T. deformans* inoculation. Principal metabolites related to the shikimic acid pathway which result modified in *P. persica* upon *T. deformans* inoculation are shown, along with the enzymes which transcripts were studied. Phenolic compounds and transcripts induction are shown indicating the genotype in which the modification is presented in at least one opportunity during the course of experiment. Only statistically significant changes are indicated. Auxin and salicylic acid are indicated with "?" since they were not measured in this work.